Cell Reports
Medicine

Report

Localization of enteroviral RNA within the pancreas in donors with T1D and T1D-associated autoantibodies

Graphical abstract

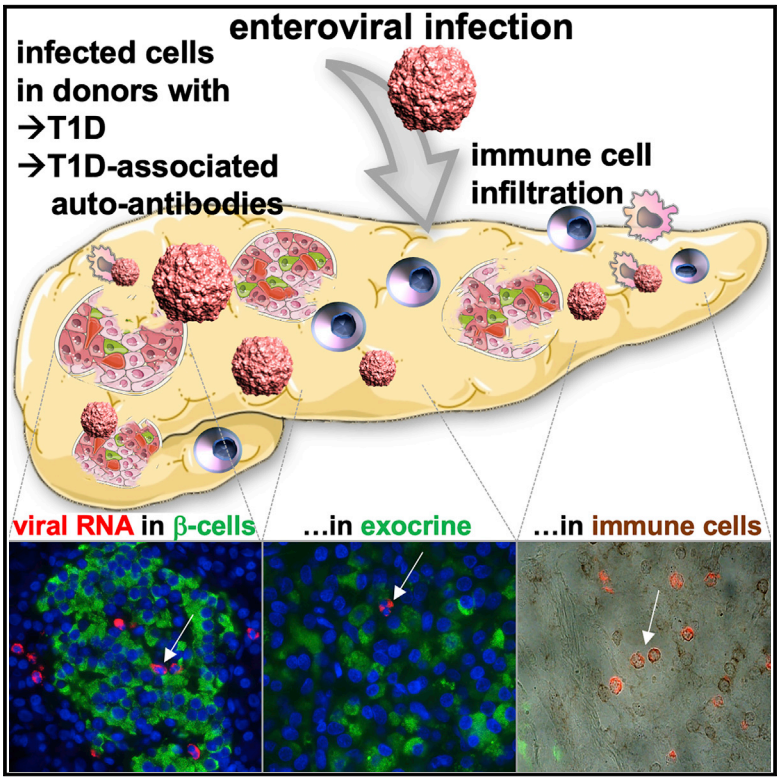

Authors

Shirin Geravandi, Sarah Richardson, Alberto Pugliese, Kathrin Maedler

Correspondence

kmaedler@uni-bremen.de

In brief

By highly sensitive, single-molecule-based fluorescent *in situ* hybridization for viral RNA, Geravandi et al. found significantly increased enterovirus-infected cells in pancreases from organ donors with type 1 diabetes (T1D) and with disease-associated autoantibodies (AAb^+), which were identified as exocrine, endocrine, and immune cells and scattered within the pancreas.

Highlights

- Enterovirus-infected cells are significantly increased in AAb^+ and T1D pancreases
- Most of the virus-positive cells are scattered within the exocrine pancreas
- Virus-positive β cells are rare but more in T1D compared to control donors
- Also elevated in T1D donors, there is more infection in spleens than in pancreases

Geravandi et al., 2021, Cell Reports Medicine *2*, 100371
August 17, 2021
https://doi.org/10.1016/j.xcrm.2021.100371

CellPress

Cell Reports Medicine

CellPress
OPEN ACCESS

Report

Localization of enteroviral RNA within the pancreas in donors with T1D and T1D-associated autoantibodies

Shirin Geravandi,[1,5,6] Sarah Richardson,[2,5] Alberto Pugliese,[3,4,5] and Kathrin Maedler[1,5,6,7,*]
[1]Centre for Biomolecular Interactions Bremen, University of Bremen, Bremen, Germany
[2]Islet Biology Group (IBEx), Exeter Centre of Excellence in Diabetes (EXCEED), University of Exeter College of Medicine and Health, Exeter, UK
[3]Diabetes Research Institute, Department of Medicine, Division of Endocrinology and Metabolism, Miami, FL, USA
[4]Department of Microbiology and Immunology, Leonard Miller School of Medicine, University of Miami, Miami, FL, USA
[5]JDRF nPOD-Virus Group
[6]Twitter: @BiologyIslet
[7]Lead contact
*Correspondence: kmaedler@uni-bremen.de
https://doi.org/10.1016/j.xcrm.2021.100371

SUMMARY

Enteroviral infections have been associated with autoimmunity and type 1 diabetes (T1D), but reliable methods to ascertain localization of single infected cells in the pancreas were missing. Using a single-molecule-based fluorescent *in situ* hybridization (smFISH) method, we detected increased virus infection in pancreases from organ donors with T1D and with disease-associated autoantibodies (AAb$^+$).

Although virus-positive β cells are found at higher frequency in T1D pancreases, compared to control donors, but are scarce, most virus-positive cells are scattered in the exocrine pancreas. Augmented CD45$^+$ lymphocytes in T1D pancreases show virus positivity or localization in close proximity to virus-positive cells. Many more infected cells were also found in spleens from T1D donors.

The overall increased proportion of virus-positive cells in the pancreas of AAb$^+$ and T1D organ donors suggests that enteroviruses are associated with immune cell infiltration, autoimmunity, and β cell destruction in both preclinical and diagnosed T1D.

INTRODUCTION

Elevated apoptotic signaling cascades, hyper-expression of histocompatibility leukocyte antigen (HLA)-I clusters, as well as islet infiltration by T cells and other immune cells represent key pathological hallmarks of type 1 diabetes (T1D), leading to interferon response and T-cell-mediated β cell destruction, impaired insulin secretion, and severe hyperglycemia.[1] A complex genetic susceptibility with polymorphisms in immune response, viral response, and β cell function genes are strong risk factors for disease development. Overall, approximately 50 loci have been linked to T1D risk.[2,3] Despite the genetic predisposition, the rapid rise in the incidence of childhood T1D worldwide, at an estimated average annual increase of 3.9% over the past decades, is too high to result only from genetic causes;[4–6] we also know from monozygotic twins that genetics do not fully explain T1D, given that disease concordance does not reach 100% (30%–70% range).[7] Earlier studies have linked T1D risk to diverse environmental factors, including epidemiological, pathological, and *in vitro* studies that have implicated enteroviruses as initiators of autoimmunity and β cell failure in genetically susceptible individuals.[1,8–10] Enteroviral infection could indeed affect the pancreas, and numerous studies show that β cells are highly susceptible to enteroviral infection *in vitro*, with subsequent activation of the interferon response pathway, upregulation of interferon (IFN)-inducible genes, massive cytokine and chemokine production, β cell death, T cell activation, and thus the triggering of autoimmunity and T1D.[11,12] Previous studies of pancreases from deceased patients with T1D have reported increased prevalence of enterovirus infections by examining the presence of the viral capsid protein (VP1)[8] by immunohistochemistry. Yet detection of enterovirus RNA in pancreas has remained challenging, in part due to limited access to suitable pancreas specimens and sensitive methodology to detect RNA. Importantly, in the Diabetes Virus Detection (DiViD) study, enterovirus was found in pancreas biopsies of newly diagnosed patients with T1D.[13] As part of the collaborative efforts of the Network for Pancreatic Organ Donors with Diabetes (nPOD)-Virus Group, an international collaborative effort that investigates the role of viruses in T1D, we aimed at examining the presence of enterovirus in pancreas samples from organ donors with and without T1D from the well-characterized human pancreatic donor tissue established by nPOD.[14] To this end, we developed a robust and highly sensitive method to detect very low amounts of virus RNA and potentially

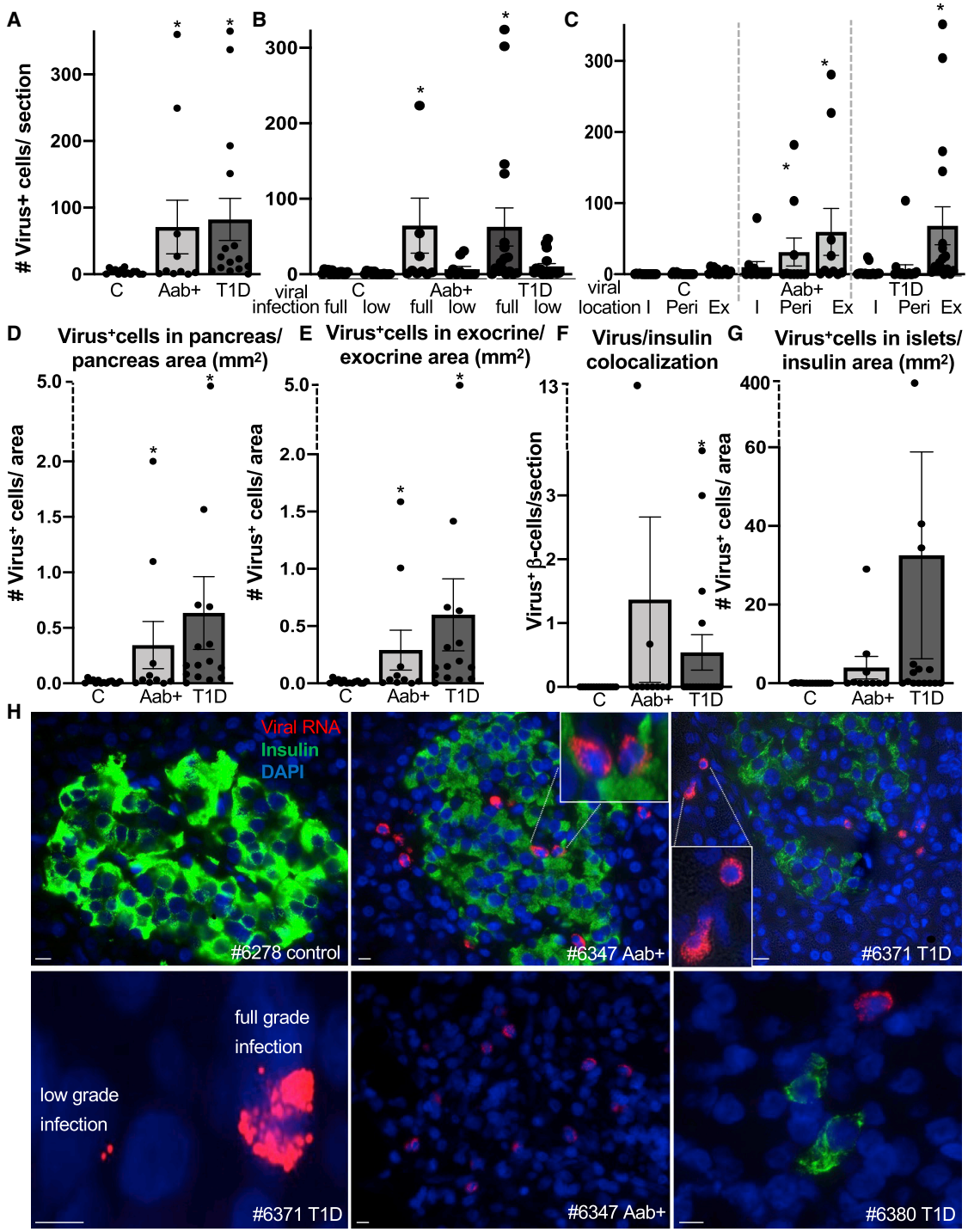

Figure 1. Pancreatic enteroviral RNA in AAb-positive and T1D patients within both the endocrine and exocrine pancreas

(A–H) Detection and quantification of viral RNA (red), insulin (green), and DAPI (blue) in FFPE pancreases from control donors without diabetes (n = 14), donors without diabetes but expressing T1D-associated autoantibodies (AAb$^+$) (n = 10), and donors with T1D (n = 15).

(A–C) Data are presented as (A) mean number of all viral RNA$^+$ cells throughout the whole pancreas section, (B) the mean number of full-grade (full; ≥10 single puncta/cell) or low-grade (low; 1–9 single puncta/cell) infected cells, and (C) their localization in the pancreas within insulin-containing islets (I), within the periphery of 3 cells of insulin-containing islets (Peri), and within the exocrine pancreas (Ex).

(D and E) All (D) viral mRNA$^+$ cells were normalized to the pancreas area of the respective section and (E) viral mRNA$^+$ cells in the exocrine area were normalized to the exocrine area of the respective section.

(legend continued on next page)

even replication-deficient virus in pancreas specimens.[15] We have previously established an adapted single-molecule *in situ* hybridization (smFISH) method that can detect single RNA molecules *in situ* using short (~20 nt) fluorescently labeled oligonucleotides, which anneal to common regions of the RNA genome of the coxsackievirus family. We successfully detected viral RNA in both cultured cells and formalin-fixed, paraffin-embedded (FFPE) samples tissue sections, in combination with classical immunostaining. Short probes were able to detect viral infection at lower viral loads than classical immunostaining and even PCR.[16,17] For initial validation, we performed several blinded concordance studies using pancreases from control and T1D patients with residual β cells, obtained from the nPOD and the Exeter (UK) cohorts.[17]

Here, we report results from an *in situ* analysis of pancreatic virus infiltration of nPOD organ donors without diabetes (control), with T1D, and with T1D-associated autoantibodies (AAb^+) without diabetes, possibly representing individuals at increased risk of future T1D. The aims of this study were (1) to identify whether there is a correlation of pancreatic enteroviral RNA expression, autoantibody positivity, and T1D and (2) to localize and characterize enteroviral infection in the pancreas.

RESULTS AND DISCUSSION

smFISH detected increased enterovirus RNA in the pancreas of T1D and AAb^+ donors

With smFISH, we successfully detected enteroviral RNA in FFPE fixed pancreases. As many of us undergo mostly asymptomatic enteroviral infections throughout life, we had initially expected to find viral RNA in all pancreases. The proportion of donors expressing enterovirus RNA in pancreatic cells were 64% (9/14) among controls, 90% (9/10) in AAb^+ donors without T1D, and 100% (15/15) among T1D donors (Tables S1–S3 for donors' demographic data).

Although control donors had a mean of 3.7 ± 1 (SE) viral RNA-containing cells in their pancreases, there were 19- and 22-fold more in pancreases from AAb^+ (mean 71 ± 40 [SE]; $p = 0.03$) and T1D donors (mean 82 ± 29 [SE]; $p = 0.01$), respectively, compared to the control group (Figure 1A).

The aggregated signal from all enteroviral probes bound to a single target molecule to produce a puncta signal requires >17 probes to bind before the observation of a fluorescence signal.[18] This allows clear single-molecule viral RNA staining and the counting of the corresponding puncta. Based on the numbers of such puncta, we classified infections as low-grade (1–9 puncta per cell) and full-grade infection (≥10 puncta per cell; Figures 1B and 1H, lower left panel; Table S1). Although there was a significant increase in low-grade infected cells in T1D donors (9-fold), the numbers of full-grade infected cells were 26-fold and 29-fold higher in AAb^+ and T1D pancreases, respectively, compared to controls (Figure 1B; Table S1). Moreover, 4/10 AAb^+ and 9/15 T1D pancreases harbored more than 10 fully infected cells containing enteroviral RNA compared to 0/14 control pancreases (Table S1). A closer look at the virus-containing cells depicts their morphological distinction from their neighbors, with loss of structured membranes and cellular disintegration (Figures S1A, S1B, S2, and S3, lower right panels), as observed in response to viral infection.[19]

Initially, probes were designed to detect the positive-stranded RNA of the entire range of group B enteroviruses.[17] In order to verify whether viruses have at least initially replicated in the cell, an additional probe set was designed to detect the negative-stranded RNA of conserved regions of the coxsackievirus B3 (CVB3) consensus-based sequence (M33854.1).[17] Such proof-of-concept approach delivered very similar results in the pancreas, namely enteroviral RNA labeling within and in proximity of the endocrine pancreas as well as scattered in the exocrine part (Figures S1C–S1F).

Pancreatic enteroviral mRNA in AAb-positive and T1D organ donors in both the endocrine and exocrine pancreas

We found a significant increase of exocrine and endocrine cells of the pancreas carrying low- and full-grade virus infections in AAb^+ and T1D, compared to controls, when we normalized to the whole pancreas area (Figure 1D). Moreover, virus-positive cells located in the exocrine pancreas normalized to the area of the exocrine pancreas were increased in AAb^+ as well as in T1D pancreases compared to controls (Figures 1E and S2).

Double staining of viral RNA with the β cell marker insulin allowed us to localize and quantify the viral RNA within β cells. Despite variation and the low number of virus-positive β cells, these were significantly more numerous among residual β cells of T1D donors (Figures 1F and 1H), compared to control donors. There was no significant difference for AAb^+ donors. Normalization of these virus-positive cells to the area of all remaining insulin-containing islets showed again a high variation and a non-significant tendency toward higher intra-islet viral RNA in T1D (Figures 1G and 1H). Based on availability of T1D donors, they were selected for the study to include donors with long (>3 years; $n = 5$) and short disease duration (<3 years; $n = 10$), with most of the donors presenting remaining insulin-containing islets (ICIs). With longer disease duration, there was a significant reduction in the number of ICIs, although the trend toward lesser virus-containing cells was not significant ($p = 0.07$; Figure S3A).

Quantification of β cells in the pancreas also confirmed the expected β cell loss in T1D: the loss in number of islets per section; the reduction in absolute β cell volume per section; as well as the percentage of insulin containing to all pancreatic cells (Figure S3B–S3D). We also found a reduction in the proportion of β cells relative to whole pancreas area in non-T1D AAb^+ organ donors from this cohort (Figures S3C and S3D), which has not been seen before in similarly small cohorts,[20–23] especially not in adult donors, who show little evidence of β cell loss.[24] Donor ages across studies may explain the difference; our study analyzed

(F and G) Viral $mRNA^+$ β cells (F) co-staining with insulin (absolute value) and viral $mRNA^+$ cells (G) within islets normalized to islet area ($insulin^+$ stained area in mm^2).

(H) Representative microscopical pictures from immunostainings of control, AAb^+, and T1D pancreatic sections. Stainings were performed in two technical replicas. Scale bars depict 10 μm. *$p<0.05$ to control.

younger AAb$^+$ donors (mean age of 20 years; Tables S2 and S3) than previous ones (mean age >30).[20–23]

These observations clearly show that enteroviruses do not exclusively target β cells but are also found in the exocrine pancreas. The observation of virus-positive cells in the exocrine pancreas may provide a pathophysiological link to previous studies reporting reduced pancreas weight in AAb$^+$ and T1D organ donors; moreover, living relatives of T1D patients with autoantibodies were reported to have a 25% reduction in pancreas weight.[25,26] Moreover, acinar loss has been reported in the T1D pancreas.[27,28] Altogether, we speculate that viral infections may contribute to pancreatic both endocrine and exocrine abnormalities that are being reported throughout the natural history of T1D.

Viral RNA is increased in lymphocytic cells in T1D

Many virus-positive cells did not stain for insulin or glucagon (Figures S3E–S3H) nor were located within or near islets and did not stain for amylase, which marks exocrine cells (Figure S2). Thus, we evaluated their co-localization with markers of ductal and immune cells and their proximity to such cells. We did find a minority of CK-19-positive and viral-positive cells within pancreatic ducts (1–3 cells/pancreas in 4 AAb$^+$ and 1–15 cells/pancreases in 6 T1D pancreases; data not shown), although no virus-positive ductal cells were observed in controls. We also found a significant increase of virus/CD45 co-positive cells in T1D pancreases, compared to nondiabetic controls, in whom no virus was found in CD45$^+$ cells (Figure 2A). Virus/CD45 co-positive cells were identified in 9 out of 15 T1D cases. Of note, such virus/CD45 co-localization was only seen in pancreases of two of three donors with dual AAb$^+$, but not among single AAb$^+$ donors (Figure 2A). T1D pancreases and these two from dual AAb$^+$ donors also presented a higher number of CD45$^+$ cells within islets as well as in the exocrine pancreas, compared to controls. There was no significant increase in CD45-lymphocyte infiltration in pancreases from single AAb$^+$ donors (Figures 2B and 2C) compared to controls. As individuals with multiple islet AAb have a higher risk of progression to T1D compared to those with a single AAb (∼80%–90% versus ∼10% in 5 years),[24] the higher pancreatic CD45-lymphocyte counts may be an indicator of more aggressive pathology. As shown by representative examples (Figures 2D, S2, S3G, and S3H), virus-positive immune cells are often found in close proximity within three cell layers to insulin$^+$ islet cells and in the exocrine pancreas. Moreover, many virus$^+$/CD45$^-$ cells were located in proximity (within three cell layers) to CD45$^+$ immune cells; further staining demonstrated some of these cells included CD4$^+$ and CD8$^+$ T cells (Figure 2D). Staining for negative-stranded enteroviral RNA confirmed viral replication in immune cells in T1D (Figure S1F). The observed increased virus load in pancreatic immune cells in dual AAb$^+$ and in T1D donors may be a starting point of the disease; further studies on T1D at-risk donors are needed to confirm such hypothesis.

Viral RNA is increased in the spleen in T1D

Well known from animal models of diabetes, the spleen harbors autoreactive T cells, as splenocytes can cause disease in adoptive transfer experiments.[29,30] Moreover, there is evidence that islet-infiltrating T cells from deceased patients are also present in the spleen.[31,32] Therefore, we investigated whether enteroviral RNA is also carried by lymphocytes in the spleen. Indeed, viral RNA was distributed throughout the spleen sections from nondiabetic controls, AAb$^+$, as well as T1D donors, with many more infected cells than seen in the pancreas (188-fold in controls and 8-fold higher both in AAb$^+$ and T1D spleens, compared to the respective pancreases; Figure 3). Quantification of virus$^+$ cells/spleen section area revealed increased virus$^+$ cells in T1D donors compared to controls (Figure 3A); virus$^+$ cells either co-stained with CD45 or were next to CD45$^+$ cells (Figure 3C), similar to what has been observed in the pancreas. The number of virus load in spleen was independent from the pancreas, as we could not find a correlation between the number of overall virus$^+$ cells in pancreas and spleen from the same patients (Figure 3B).

Increased enteroviral RNA found in the spleen in T1D is also in line with identified enteroviral RNA in peripheral blood mononuclear cells (PBMCs) from patients with recent onset as well as long-term T1D.[33–36] Enterovirus presence in T1D-PBMCs is linked with the T1D risk allele HLA-DR4, carried by all virus-positive patients in this previous study.[35] Such correlations are difficult to predict from a small number of patients, as also in 4 out of 10 patients, no virus was identified in PBMCs in this previous study. Also in our cohort, the limited sample size prevented reaching conclusions about possible associations between splenic or pancreatic virus loads and T1D HLA-risk alleles. Although a double AAb$^+$ donor with the virus load >200 infected cells in the pancreas had the high-risk alleles HLA-DRB1*03 (DR3) and DQB1*03:02 (DQ8), neither another double AAb$^+$ donor nor another single AAb$^+$ donor with >300 infected cells had the same high-risk alleles. Similarly, some T1D donors with large numbers of infected cells had the high-risk alleles, which contrasts to another donor with the same risk alleles but with a relatively lower number of infected cells (Table S3).

Overall, we found increased presence of enteroviral RNA-positive cells in the pancreas of organ donors with T1D-associated autoantibodies (without T1D) and with T1D, many of which had a short disease duration and presented remaining insulin-containing islets, suggesting an ongoing disease process. This was enabled through a highly sensitive and specific RNA detection down to a single RNA molecule in well-preserved FFPE pancreases with the advantage of spatial cellular localization of viral RNA at a single-cell level. Previous studies were limited to VP1 staining with much lower sensitivity,[17] as well as to PCR, although with similar sensitivity, its limitation lies in the low accessibility and stability of nucleic acids through RNA degradation in the pancreas.

Enteroviral RNA-infected cells could be located within the endocrine and the exocrine pancreas; their appearance as well as the close proximity to immune cells suggest virus-induced immune cell attraction and infiltration. Viruses in multiple cell types in the pancreas highlight their various impacts on diabetes pathology, affecting the β cell, exocrine, and immune cells. What signal is transferred from an infected immune cell? One can speculate that it has either already transferred the virus to islets or will do so soon.

The presence of enteroviral RNA in nondiabetic AAb$^+$ donors is in line with previous studies that have detected viral infection in

CellPress
OPEN ACCESS

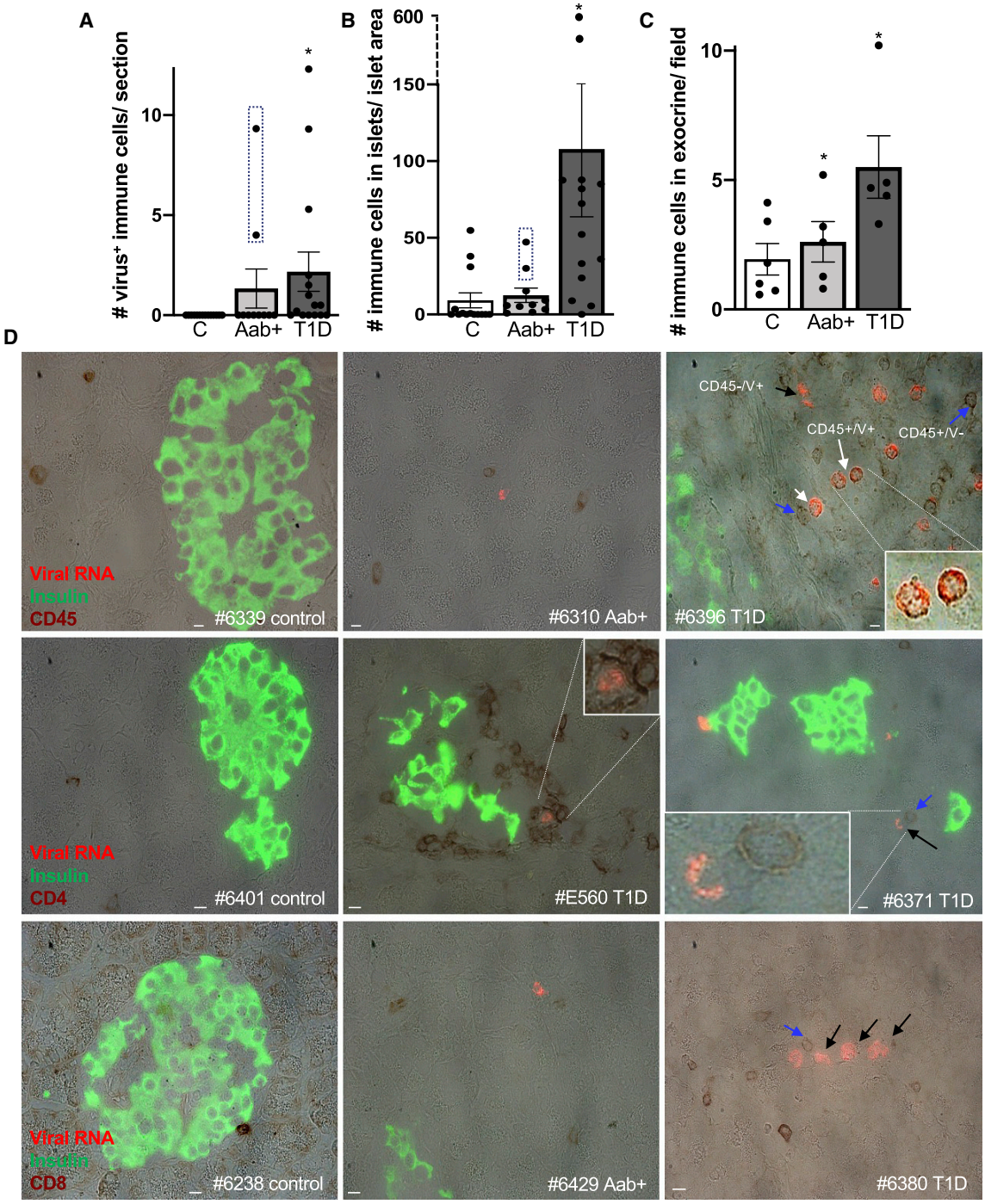

Figure 2. Enteroviral RNA is increased in lymphocytic cells in T1D

(A–D) Detection and quantification of viral RNA (red), insulin (green), and CD45, CD4, or CD8 in bright field (dark red) in FFPE pancreases from autopsy from control donors without diabetes (A, B, and D: n = 14; C: n = 6), with T1D-associated autoantibodies (A, B, and D: AAb$^+$, n = 10; C: n = 5), and with T1D (A, B, and D: n = 15; C: n = 5) and presented as (A) mean number of viral RNA$^+$/CD45 co-positive cells throughout the whole pancreas section and (B) quantification of CD45 co-positive cells within insulin-containing islets and (C) within the exocrine pancreas. 15 randomly chosen parts of equal size of each pancreas section were analyzed. The dashed boxes in (A) and (B) mark two donors of the study cohort with dual AAb$^+$, showing increased virus/CD45 co-localization (A) and CD45$^+$ cells within islets (B), compared to controls and single AAb$^+$ donors.

(D) Representative microscopical pictures from immunostainings of control, AAb$^+$, and T1D pancreatic sections. White arrows show viral RNA$^+$/CD45$^+$ co-positive cells, black arrows viral RNA$^+$/CD45$^-$ cells, and blue arrows viral RNA$^-$/CD45$^+$ cells next to a viral RNA$^+$ cell. Stainings were performed in two technical replicas. Scale bars depict 10 μm. *p<0.05 to control.

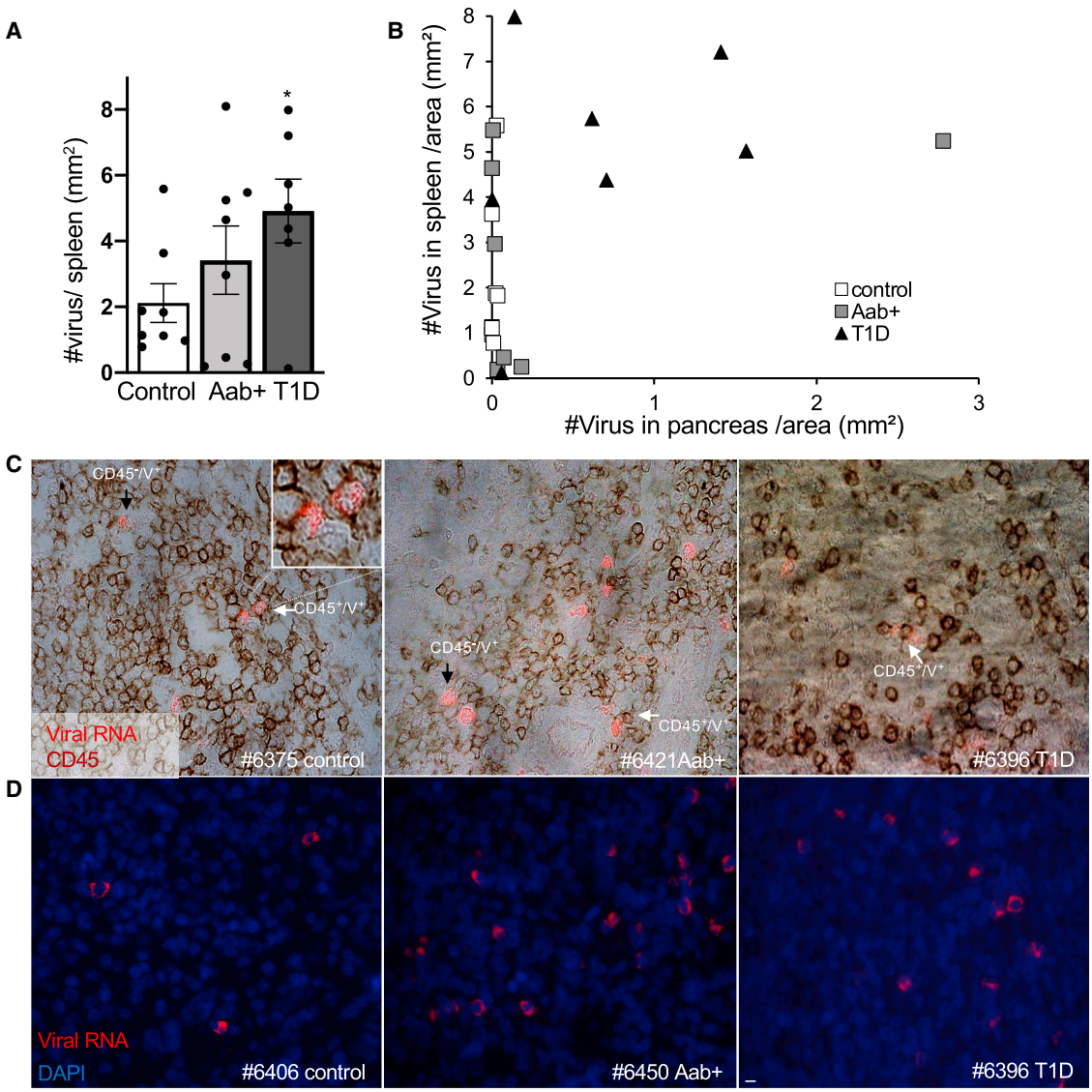

Figure 3. Enteroviral RNA is increased in the spleen in T1D

(A and B) Detection and quantification of viral RNA (red), CD45 in bright field (dark red), and DAPI in blue in FFPE spleen sections from autopsy from a subset of the analyzed pancreas donors without diabetes (n = 8), with T1D-associated autoantibodies (AAb$^+$) (n = 8), and with T1D (n = 7) and presented as (A) mean number of viral RNA$^+$ cells/spleen section area and (B) a correlation of the mean number of viral RNA$^+$ cells/spleen section area with the mean number of viral RNA$^+$ cells/pancreas section area. (C and D) Representative microscopical pictures from immunostainings of control, AAb$^+$, and T1D pancreatic sections of viral RNA/CD45 double staining (C) and viral RNA/DAPI double staining (D). White arrows show viral RNA$^+$/CD45$^+$ co-positive cells and black arrows viral RNA$^+$/CD45$^-$ cells next to CD45$^+$ cells. Stainings were performed in two technical replicas. Scale bars depict 10 μm. *p<0.05 to control.

children at risk for T1D.[1,37–39] Multiple enteroviral infection rounds through early childhood may trigger the disease,[39] and as seen here, viral sequences remain in the tissue for years after infection, having either been among the initiating or participating factors toward the damage of the pancreas and the vulnerable β cell.

Limitations of study

Although we could clearly observe increased enteroviral infection in spleens and pancreases in organ donors with T1D, the small sample size did not allow a correlation of virus load with other strong predictors of autoimmunity or T1D severity, e.g., with HLA phenotype, number of autoantibodies, disease duration, or age of T1D diagnosis. Furthermore, our broad approach in the enteroviral probe design did not enable identification of specific viral sequences. Using smFISH, larger studies are needed for the identification of the specific viral infection association with autoimmunity and T1D.

STAR★METHODS

Detailed methods are provided in the online version of this paper and include the following:

SUPPLEMENTAL INFORMATION

Supplemental information can be found online at https://doi.org/10.1016/j.xcrm.2021.100371.

ACKNOWLEDGMENTS

This research was only possible with the support of the Network for Pancreatic Organ Donors with Diabetes (nPOD), a collaborative type 1 diabetes research project sponsored by JDRF. Organ Procurement Organizations (OPOs) partnering with nPOD to provide research resources are listed at https://www.jdrfnpod.org/for-partners/npod-partners/. We express our deep gratitude to the donors and their families. We also thank our colleagues from the nPOD viral working group (nPOD-V) for encouragement and discussion throughout this study and especially Irina Kusmartseva (University of Florida, Miami) for help with donor procurement for this study and Richard E. Lloyd (Baylor College of Medicine) for kindly providing the enterovirus image for the graphical abstract. We acknowledge Amin Ardestani for being a great mentor for all undergrad and grad students in the lab and his great suggestions for the normalization of the results in this study. We would like to thank Katrischa Hennekens for excellent technical assistance and Alaa Issawi (all Uni Bremen) for establishing the virus-amylase co-staining. This study was supported by JDRF to the nPOD-Virus Group (JDRF SRA-5-2012-516 and JDRF 3-SRA-2017-492-A-N; head-PI: A.P.; University of Miami) and by the German Research Foundation (DFG; to K.M.). The funders had no role in study design, data collection and analysis, decision to publish, or preparation of the manuscript.

AUTHOR CONTRIBUTIONS

S.G. performed experiments, analyzed data, and wrote the paper. S.R. provided intellectual support and pathological specimen. A.P. provided intellectual support, pathological specimen, and demographic data and wrote the paper. K.M. designed and performed experiments, analyzed data, supervised the project, and wrote the paper.

DECLARATION OF INTERESTS

The authors declare no competing interests.

INCLUSION AND DIVERSITY

We worked to ensure gender and ethnicity balance regarding the scientists who initiated and performed this study and regarding the assignment of organ donors for this study.

Received: February 22, 2021
Revised: June 7, 2021
Accepted: July 19, 2021
Published: August 17, 2021

REFERENCES

1. Geravandi, S., Liu, H., and Maedler, K. (2020). Enteroviruses and T1D: is it the virus, the genes or both which cause T1D. Microorganisms *8*, E1017.
2. Barrett, J.C., Clayton, D.G., Concannon, P., Akolkar, B., Cooper, J.D., Erlich, H.A., Julier, C., Morahan, G., Nerup, J., Nierras, C., et al.; Type 1 Diabetes Genetics Consortium (2009). Genome-wide association study and meta-analysis find that over 40 loci affect risk of type 1 diabetes. Nat. Genet. *41*, 703–707.
3. Robertson, C.C., Inshaw, J.R.J., Onengut-Gumuscu, S., Chen, W.M., Santa Cruz, D.F., Yang, H., Cutler, A.J., Crouch, D.J.M., Farber, E., Bridges, S.L., Jr., et al.; Type 1 Diabetes Genetics Consortium (2021). Fine-mapping, trans-ancestral and genomic analyses identify causal variants, cells, genes and drug targets for type 1 diabetes. Nat. Genet. *53*, 962–971.
4. Hyöty, H., and Taylor, K.W. (2002). The role of viruses in human diabetes. Diabetologia *45*, 1353–1361.
5. Yeung, W.C., Rawlinson, W.D., and Craig, M.E. (2011). Enterovirus infection and type 1 diabetes mellitus: systematic review and meta-analysis of observational molecular studies. BMJ *342*, d35.
6. Oikarinen, M., Tauriainen, S., Oikarinen, S., Honkanen, T., Collin, P., Rantala, I., Mäki, M., Kaukinen, K., and Hyöty, H. (2012). Type 1 diabetes is associated with enterovirus infection in gut mucosa. Diabetes *61*, 687–691.
7. Jerram, S.T., and Leslie, R.D. (2017). The genetic architecture of type 1 diabetes. Genes (Basel) *8*, E209.
8. Morgan, N.G., and Richardson, S.J. (2014). Enteroviruses as causative agents in type 1 diabetes: loose ends or lost cause? Trends Endocrinol. Metab. *25*, 611–619.
9. Hober, D., and Alidjinou, E.K. (2013). Enteroviral pathogenesis of type 1 diabetes: queries and answers. Curr. Opin. Infect. Dis. *26*, 263–269.
10. Hober, D., and Sane, F. (2010). Enteroviral pathogenesis of type 1 diabetes. Discov. Med. *10*, 151–160.
11. Marroqui, L., Lopes, M., dos Santos, R.S., Grieco, F.A., Roivainen, M., Richardson, S.J., Morgan, N.G., Op de Beeck, A., and Eizirik, D.L. (2015). Differential cell autonomous responses determine the outcome of coxsackievirus infections in murine pancreatic α and β cells. eLife *4*, e06990.
12. Schulte, B.M., Lanke, K.H., Piganelli, J.D., Kers-Rebel, E.D., Bottino, R., Trucco, M., Huijbens, R.J., Radstake, T.R., Engelse, M.A., de Koning, E.J., et al. (2012). Cytokine and chemokine production by human pancreatic islets upon enterovirus infection. Diabetes *61*, 2030–2036.
13. Krogvold, L., Edwin, B., Buanes, T., Frisk, G., Skog, O., Anagandula, M., Korsgren, O., Undlien, D., Eike, M.C., Richardson, S.J., et al. (2015). Detection of a low-grade enteroviral infection in the islets of langerhans of living patients newly diagnosed with type 1 diabetes. Diabetes *64*, 1682–1687.
14. Laiho, J.E., Oikarinen, S., Oikarinen, M., Larsson, P.G., Stone, V.M., Hober, D., Oberste, S., Flodström-Tullberg, M., Isola, J., and Hyöty, H. (2015). Application of bioinformatics in probe design enables detection of enteroviruses on different taxonomic levels by advanced in situ hybridization technology. J. Clin. Virol. *69*, 165–171.
15. Tracy, S., Smithee, S., Alhazmi, A., and Chapman, N. (2015). Coxsackievirus can persist in murine pancreas by deletion of 5′ terminal genomic sequences. J. Med. Virol. *87*, 240–247.
16. Laiho, J.E., Oikarinen, M., Richardson, S.J., Frisk, G., Nyalwidhe, J., Burch, T.C., Morris, M.A., Oikarinen, S., Pugliese, A., Dotta, F., et al.; JDRF nPOD-Virus Group (2016). Relative sensitivity of immunohistochemistry, multiple reaction monitoring mass spectrometry, in situ hybridization and PCR to detect Coxsackievirus B1 in A549 cells. J. Clin. Virol. *77*, 21–28.
17. Busse, N., Paroni, F., Richardson, S.J., Laiho, J.E., Oikarinen, M., Frisk, G., Hyöty, H., de Koning, E., Morgan, N.G., and Maedler, K. (2017). Detection and localization of viral infection in the pancreas of patients with type 1

diabetes using short fluorescently-labelled oligonucleotide probes. Oncotarget *8*, 12620–12636.

18. Raj, A., van den Bogaard, P., Rifkin, S.A., van Oudenaarden, A., and Tyagi, S. (2008). Imaging individual mRNA molecules using multiple singly labeled probes. Nat. Methods *5*, 877–879.
19. Hodik, M., Skog, O., Lukinius, A., Isaza-Correa, J.M., Kuipers, J., Giepmans, B.N., and Frisk, G. (2016). Enterovirus infection of human islets of Langerhans affects β-cell function resulting in disintegrated islets, decreased glucose stimulated insulin secretion and loss of Golgi structure. BMJ Open Diabetes Res. Care *4*, e000179.
20. Rodriguez-Calvo, T., Richardson, S.J., and Pugliese, A. (2018). Pancreas pathology during the natural history of type 1 diabetes. Curr. Diab. Rep. *18*, 124.
21. Campbell-Thompson, M., Fu, A., Kaddis, J.S., Wasserfall, C., Schatz, D.A., Pugliese, A., and Atkinson, M.A. (2016). Insulitis and β-cell mass in the natural history of type 1 diabetes. Diabetes *65*, 719–731.
22. In't Veld, P., Lievens, D., De Grijse, J., Ling, Z., Van der Auwera, B., Pipeleers-Marichal, M., Gorus, F., and Pipeleers, D. (2007). Screening for insulitis in adult autoantibody-positive organ donors. Diabetes *56*, 2400–2404.
23. Rodriguez-Calvo, T., Ekwall, O., Amirian, N., Zapardiel-Gonzalo, J., and von Herrath, M.G. (2014). Increased immune cell infiltration of the exocrine pancreas: a possible contribution to the pathogenesis of type 1 diabetes. Diabetes *63*, 3880–3890.
24. Leslie, R.D., Atkinson, M.A., and Notkins, A.L. (1999). Autoantigens IA-2 and GAD in type I (insulin-dependent) diabetes. Diabetologia *42*, 3–14.
25. Campbell-Thompson, M., Wasserfall, C., Montgomery, E.L., Atkinson, M.A., and Kaddis, J.S. (2012). Pancreas organ weight in individuals with disease-associated autoantibodies at risk for type 1 diabetes. JAMA *308*, 2337–2339.
26. Campbell-Thompson, M.L., Filipp, S.L., Grajo, J.R., Nambam, B., Beegle, R., Middlebrooks, E.H., Gurka, M.J., Atkinson, M.A., Schatz, D.A., and Haller, M.J. (2019). Relative pancreas volume is reduced in first-degree relatives of patients with type 1 diabetes. Diabetes Care *42*, 281–287.
27. Wright, J.J., Saunders, D.C., Dai, C., Poffenberger, G., Cairns, B., Serreze, D.V., Harlan, D.M., Bottino, R., Brissova, M., and Powers, A.C. (2020). Decreased pancreatic acinar cell number in type 1 diabetes. Diabetologia *63*, 1418–1423.
28. Kusmartseva, I., Beery, M., Hiller, H., Padilla, M., Selman, S., Posgai, A., Nick, H.S., Campbell-Thompson, M., Schatz, D.A., Haller, M.J., et al. (2020). Temporal analysis of amylase expression in control, autoantibody-positive, and type 1 diabetes pancreatic tissues. Diabetes *69*, 60–66.
29. Wicker, L.S., Miller, B.J., and Mullen, Y. (1986). Transfer of autoimmune diabetes mellitus with splenocytes from nonobese diabetic (NOD) mice. Diabetes *35*, 855–860.
30. Höglund, P., Mintern, J., Waltzinger, C., Heath, W., Benoist, C., and Mathis, D. (1999). Initiation of autoimmune diabetes by developmentally regulated presentation of islet cell antigens in the pancreatic lymph nodes. J. Exp. Med. *189*, 331–339.
31. Codina-Busqueta, E., Scholz, E., Muñoz-Torres, P.M., Roura-Mir, C., Costa, M., Xufré, C., Planas, R., Vives-Pi, M., Jaraquemada, D., and Martí, M. (2011). TCR bias of in vivo expanded T cells in pancreatic islets and spleen at the onset in human type 1 diabetes. J. Immunol. *186*, 3787–3797.
32. Seay, H.R., Yusko, E., Rothweiler, S.J., Zhang, L., Posgai, A.L., Campbell-Thompson, M., Vignali, M., Emerson, R.O., Kaddis, J.S., Ko, D., et al. (2016). Tissue distribution and clonal diversity of the T and B cell repertoire in type 1 diabetes. JCI Insight *1*, e88242.
33. Alidjinou, E.K., Chehadeh, W., Weill, J., Vantyghem, M.C., Stuckens, C., Decoster, A., Hober, C., and Hober, D. (2015). Monocytes of patients with type 1 diabetes harbour enterovirus RNA. Eur. J. Clin. Invest. *45*, 918–924.
34. Dechaumes, A., Bertin, A., Sane, F., Levet, S., Varghese, J., Charvet, B., Gmyr, V., Kerr-Conte, J., Pierquin, J., Arunkumar, G., et al. (2020). Coxsackievirus-B4 infection can induce the expression of human endogenous retrovirus W in primary cells. Microorganisms *8*, E1335.
35. Schulte, B.M., Bakkers, J., Lanke, K.H., Melchers, W.J., Westerlaken, C., Allebes, W., Aanstoot, H.J., Bruining, G.J., Adema, G.J., Van Kuppeveld, F.J., and Galama, J.M. (2010). Detection of enterovirus RNA in peripheral blood mononuclear cells of type 1 diabetic patients beyond the stage of acute infection. Viral Immunol. *23*, 99–104.
36. Yin, H., Berg, A.K., Tuvemo, T., and Frisk, G. (2002). Enterovirus RNA is found in peripheral blood mononuclear cells in a majority of type 1 diabetic children at onset. Diabetes *51*, 1964–1971.
37. Rodriguez-Calvo, T. (2018). Enteroviral infections as a trigger for type 1 diabetes. Curr. Diab. Rep. *18*, 106.
38. Stene, L.C., Oikarinen, S., Hyöty, H., Barriga, K.J., Norris, J.M., Klingensmith, G., Hutton, J.C., Erlich, H.A., Eisenbarth, G.S., and Rewers, M. (2010). Enterovirus infection and progression from islet autoimmunity to type 1 diabetes: the Diabetes and Autoimmunity Study in the Young (DAISY). Diabetes *59*, 3174–3180.
39. Vehik, K., Lynch, K.F., Wong, M.C., Tian, X., Ross, M.C., Gibbs, R.A., Ajami, N.J., Petrosino, J.F., Rewers, M., Toppari, J., et al.; TEDDY Study Group (2019). Prospective virome analyses in young children at increased genetic risk for type 1 diabetes. Nat. Med. *25*, 1865–1872.
40. Kaddis, J.S., Pugliese, A., and Atkinson, M.A. (2015). A run on the biobank: what have we learned about type 1 diabetes from the nPOD tissue repository? Curr. Opin. Endocrinol. Diabetes Obes. *22*, 290–295.
41. Foulis, A.K., Liddle, C.N., Farquharson, M.A., Richmond, J.A., and Weir, R.S. (1986). The histopathology of the pancreas in type 1 (insulin-dependent) diabetes mellitus: a 25-year review of deaths in patients under 20 years of age in the United Kingdom. Diabetologia *29*, 267–274.
42. Skog, O., Ingvast, S., and Korsgren, O. (2014). Evaluation of RT-PCR and immunohistochemistry as tools for detection of enterovirus in the human pancreas and islets of Langerhans. J. Clin. Virol. *61*, 242–247.
43. Ardestani, A., Li, S., Annamalai, K., Lupse, B., Geravandi, S., Dobrowolski, A., Yu, S., Zhu, S., Baguley, T.D., Surakattula, M., et al. (2019). Neratinib protects pancreatic beta cells in diabetes. Nat. Commun. *10*, 5015.

STAR★METHODS

KEY RESOURCES TABLE

REAGENT or RESOURCE	SOURCE	IDENTIFIER
Antibodies		
guinea pig anti-insulin	Dako; now Agilent, Santa C#lara, CA, USA	#A0546; RRID:AB_2617169
rabbit anti-glucagon		#A0565; RRID:AB_10013726
mouse anti-CD45		#M0701; RRID:AB_2314143
rabbit anti-amylase	Abcam, UK	#21156; RRID:AB_446061
rabbit anti-CD4		#133616; RRID:AB_2750883
rabbit anti-CD8		#4055; RRID:AB_304247
biotin- conjugated donkey anti-rabbit	Jackson Immuno Research, PA, USA	#711-066-152; RRID:AB_2340594
biotin- conjugated donkey anti-mouse		#715-065-150; RRID:AB_2307438
biotin- conjugated donkey anti- guinea pig		#706-066-148; RRID:AB_2340452
FITC-conjugated donkey anti-rabbit		#711-096-152; RRID:AB_2340597
FITC-conjugated donkey anti-guinea pig		#706-096-148; RRID:AB_2340454
Biological samples		
Human FFPE pancreatic sections from organ donors	this paper; Kaddis et al.[40] and Foulis et al.[41]	N/A
Chemicals, peptides, and recombinant proteins		
Sudan Black	Sigma-Aldrich	#199664
Pepsin	Sigma-Aldrich	#MKCN5185
Critical commercial assays		
VECTASTAIN ABC Kit	Vector Labs, USA	#PK-4000
DAB Peroxidase Substrate Kit		#SK-4100
VECTASHIELD® with 4',6-Diamidin-2-phenylindol (DAPI)		#H-1200-10
Oligonucleotides		
Sequences of probes and respective viral target regions of probes sets CVB_1, CVB_2, CVB_3	Designed with Stellaris® RNA FISH Probe Designer (Biosearch Technologies, Inc., Petaluma, CA)	This paper; See Table S3, Busse et al.[17]
Software and algorithms		
Vision Works LS Image Acquisition and Analysis software Version 6.8	UVP BioImaging Systems, CA, USA	N/A
NIS-Elements software, v3.22.11	Nikon GmbH, Germany	N/A
GraphPad Prism v8.4.3	GraphPad	N/A
ImageJ (v.1.52(100)	NIH, USA	N/A
Other		
Nikon MEA53200	Nikon GmbH, Germany	N/A

RESOURCE AVAILABILITY

Lead contact

Further information and requests for resources and reagents should be directed to and will be fulfilled by the lead contact, Kathrin Maedler (kmaedler@uni-bremen.de)

Materials availability

This study did not generate new unique reagents.

Data and code availability

Original/source data in the paper are available in Tables S1 and S3. This study did not generate any unique datasets or code.

EXPERIMENTAL MODELS AND SUBJECT DETAILS

Organ donor cohort and virus detection in FFPE tissue samples

Our study of organ donors included 15 with T1D (average disease duration 4 years, range 0-23 years), 10 autoantibody-positive (AAb+) donors without diabetes, and 14 control donors (without diabetes, autoantibody-negative). Key demographic features are described in Table S2. Formalin-fixed paraffin-embedded pancreatic and spleen tissue sections were obtained from well-characterized organ donors from the network for Pancreatic Organ Donors with diabetes (nPOD)[40] and from a UK cohort[41]. Detection of viral RNA was performed using custom Stellaris® FISH Probes, as described in detail in the supplemental methods and previously[17].

Study approval

Ethical approval for the use of human pancreatic tissue had been granted by the Ethics Committee of the University of Bremen. The study complied with all relevant ethical regulations for work with human tissue for research purposes. Organ donors are not identifiable and anonymous, such approved analyses using tissue for research is covered by the NIH Exemption 4 (Regulation PHS 398).

METHOD DETAILS

Virus detection in FFPE tissue samples

Custom Stellaris® FISH Probes, each recognizing various enteroviral strains, labeled with Quasar 570 were purchased from Biosearch Technologies, Inc. (Petaluma, CA) as described previously[17]. Three probes sets were used for positive strand enteroviral RNA detection, CVB_1 designed on the CVB3 consensus-based sequence (M33854.1) and for CVB_2 and CVB_3, 106 genome sequences of viruses belonging to the enterovirus group B family were aligned and divided into three subgroups based on sequence similarities. For each subgroup probes were designed based on newly generated consensus sequences as described before[42] and were distributed throughout the whole target genome. For negative strand enteroviral RNA detection, the CVB_1 set in the 3'-5'orientation was used.

Enterovirus mRNA detection was carried out by smFISH according to a previously established highly sensitive protocol[17].

Deparaffinization of FFPE Tissue sections. Residual paraffin particles and wax crystals from the embedding procedure were removed by a series of Xylene washes (20 min at 70°C; 10 min at 70°C; 10 min at room temperature), followed by rehydration by ethanol (EtOH; 100%, 100%, 95%) for 10 min each and for 1 h in 70% EtOH at room temperature. Finally, sections were rehydrated by washing with RNase free water 2 times for 2 min. All steps were performed with constant steering.

Prehybridization. Sections were incubated with 0.2M HCl for 20 min at room temperature, transferred to a 50 mL tube containing prewarmed 2xSSC and incubated in a shaking water bath at 70°C for 15 min. The sections were then washed with PBS two times for 2 min at room temperature, then incubated with prewarmed (37°C) pepsin (Sigma) for 10 min at 37°C. The sections were then washed 2 times with PBS for 1 minute at room temperature then with 0.5% Sudan Black (Sigma-Aldrich) diluted in 70% EtOH for 20 min at room temperature in order to quench any remaining autofluorescence from islets. Sections were then washed with PBS (3 times for 5 min at room temperature), then 2 times with washing buffer (1xSSC,10% formamide) for 5 min at room temperature.

Hybridization. Stellaris® FISH Probes (viral RNA 0.25 μM) were diluted 1:100 in hybridization buffer (10% w/v Dextran sulfate, 10% formamide, 2xSSC). 50 μL of all three diluted probe sets were applied to the sections, covered with a glass and kept at 37°C overnight in a humidified chamber.

Post hybridization wash. Coverslip was removed using 2xSSC, 10% formamide prewarmed to 37°C. Sections were then washed with 37°C prewarmed solution in a shaking water bath at 37°C, centrifuged shortly between each wash in an empty tube to remove washing liquid. Washing steps were as follows: 2 times 2xSSC+10% formamide for 20 min, 2 times with 2xSSC for 15 min, followed by 2 times wash with 1xSSC for 15 min, then with 0.1xSSC for 15 min and lastly with 0.1xSSC for 5 min.

One day after smFISH, pancreas sections were co-stained by classical immunostaining[43] for insulin (Dako#A0546), the exocrine acinar marker amylase (Abcam#21156), the general lymphocyte marker CD45 (Dako#M0701), and the T cell activation markers CD4 (Abcam#133616) and CD8 (Abcam#4055). All spleen sections were co-stained for CD45.

VECTASHIELD® antifade mounting medium (Vector laboratories) including 4',6-Diamidin-2-phenylindol (DAPI) was immediately added and images were acquired with a Nikon Ti MEA53200 (NIKON GmbH, Düsseldorf, Germany) microscope. A 60x oil-immersion objective was used to acquire images of the Quasar 570 labeled probes. Control images were always taken with the FITC filter at the same exposure time to ensure no false-positive signals caused by a bleed-through from one channel to another.

QUANTIFICATION AND STATISTICAL ANALYSIS

Quantification of cells and tissues

Morphometrical measurement of enteroviral mRNA, insulin, CD4, CD8, CD45, CD68 and amylase and the respective pancreatic and splenic tissue area was carried out using a NikonTiMEA53200 (NIKON GmbH, Düsseldorf, Germany) microscope. NIS-Elements BR

software (NIKON GmbH, Düsseldorf, Germany) and ImageJ (NIH, USA) were used for image analysis. Number of virus infected cells (single infected with 1-10 puncta or fully infected with $\geq$ 10 puncta), number of islets and immune cells were counted manually throughout the whole sections. Immune cells within the exocrine part of the pancreas were counted in 15 randomly selected areas of equal size for each pancreas slide. Mean percentage of the β-cell area per pancreas was calculated as the ratio of insulin-positive to whole pancreatic tissue area. The exocrine area was calculated as whole insulin-positive area subtracted from whole pancreas area. ''Islet periphery'' was defined as signal localization within 3 cell layers of insulin containing islets, and ''close proximity'' as signal localization within 3 cell layers to the respective islet cells or immune cells.

Statistical analyses

All biological replica referred to ''n'' for each individual human pancreas, which are means of two technical replica from independent staining analyses and presented as means ± SEM. Mean differences were determined by Student's t tests. A p value < 0.05 was considered statistically significant. Investigators were blinded to the cases during staining and microscopical analysis.

Cell Reports Medicine, Volume *2*

Supplemental information

Localization of enteroviral RNA within the pancreas in donors with T1D and T1D-associated autoantibodies

Shirin Geravandi, Sarah Richardson, Alberto Pugliese, and Kathrin Maedler

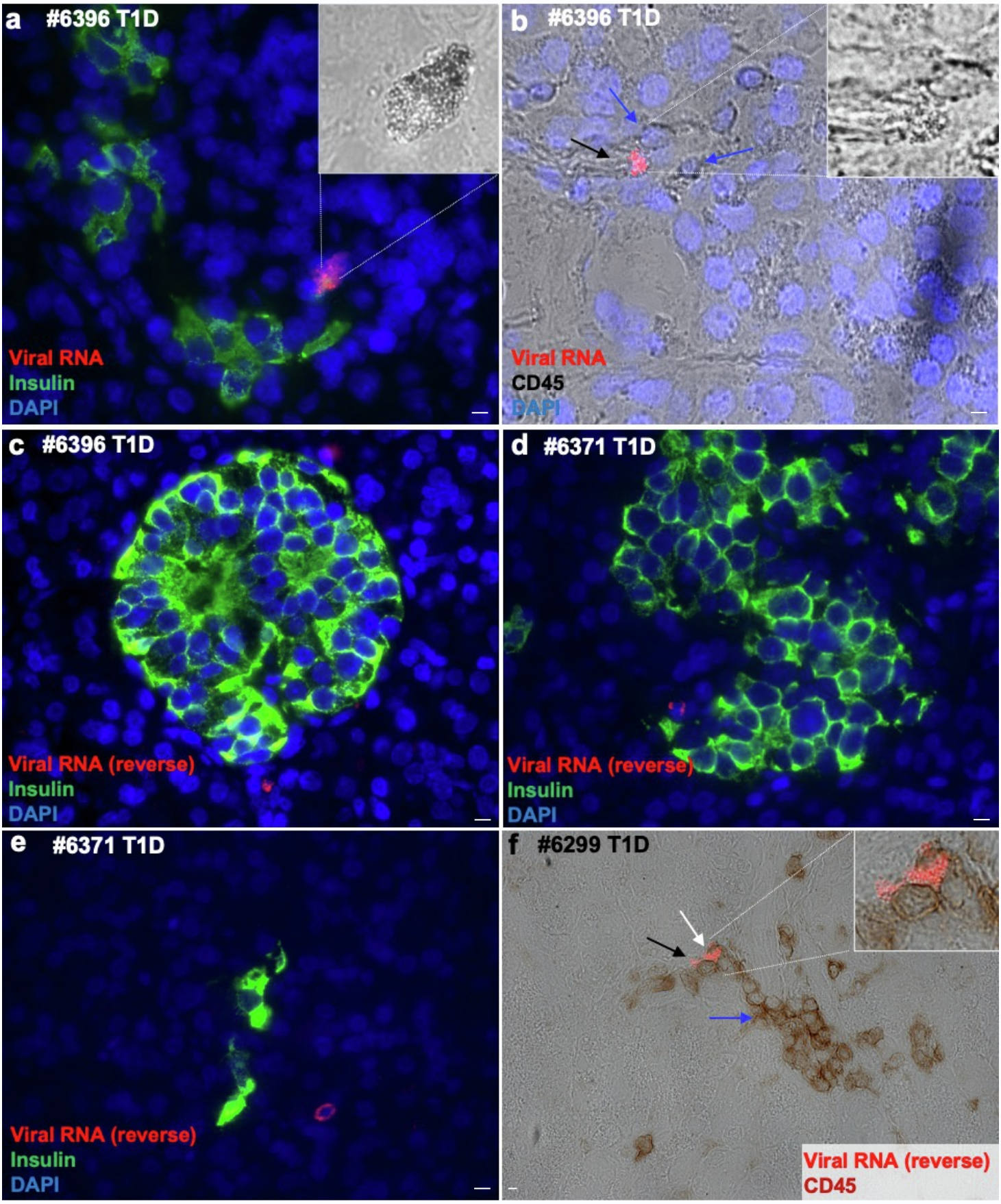

Supplemental Figure 1. Enteroviral RNA$^+$ cells with disrupted morphology and negative-stranded enteroviral RNA$^+$ cells in the pancreas. Related to Fig.1. **A,B)** Representative microscopical pictures from immunostainings of T1D (n=15, performed in two technical replica) pancreatic sections stained for viral RNA, insulin and DAPI **(A)** or stained for viral RNA, CD45 and DAPI **(B)**. Magnification of viral RNA$^+$ cells with their typical disrupted morphology (**A,B;** inserts). **(C-F)** Representative microscopical pictures from immunostainings of pancreatic sections from T1D (n=5) donors triple-stained for the negative strand of viral RNA (reverse), insulin and DAPI **(C-E)** or double-stained for viral RNA and CD45 **(F)**. White arrows show viral RNA$^+$/CD45$^+$ co-positive cells (magnified insert in **F**), black arrows viral RNA$^+$/CD45$^-$ cells, and blue arrows viral RNA$^-$/CD45$^+$ cells. Scale bars depict 10µm.

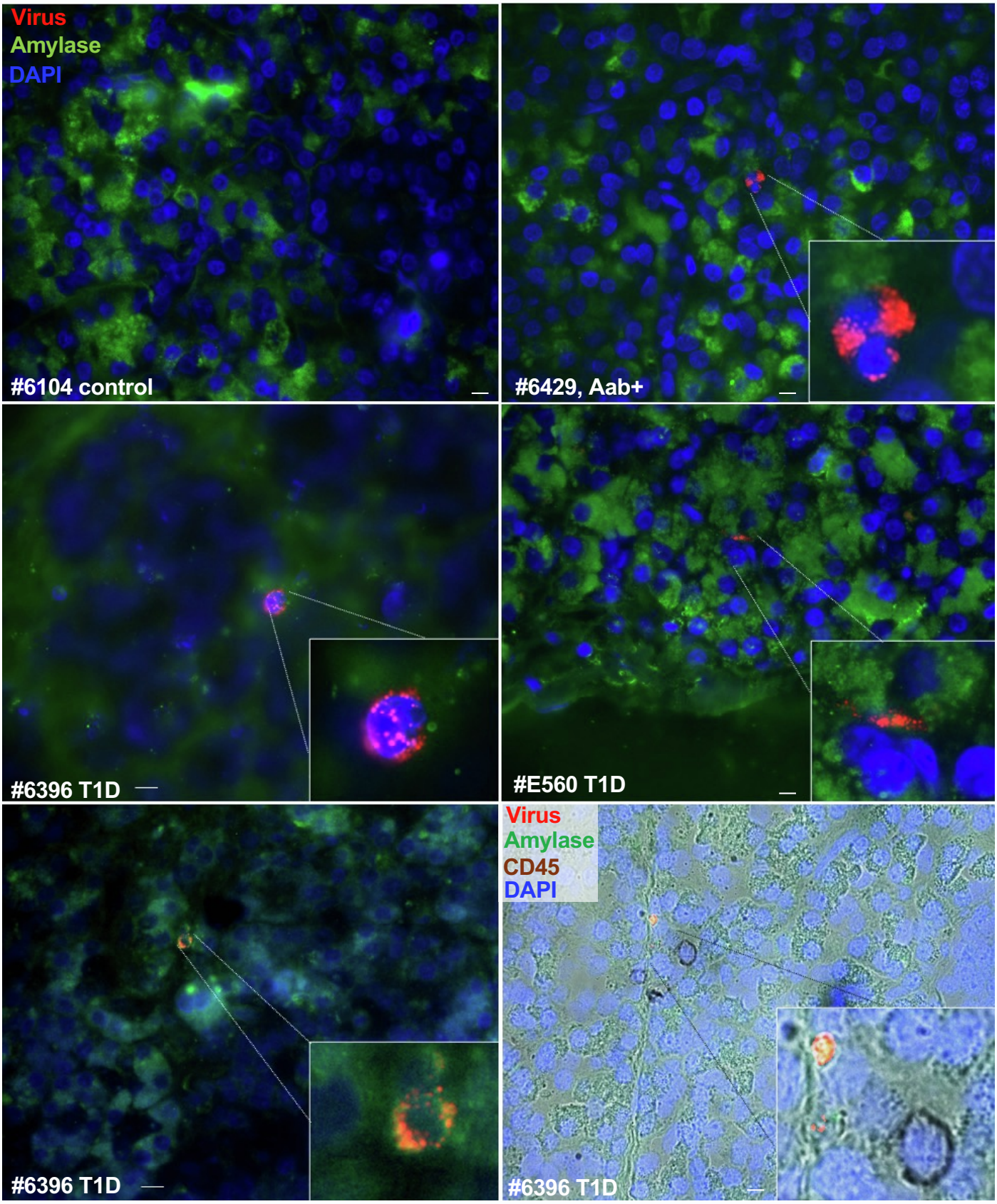

Supplemental Figure 2. Viral RNA$^+$ cells within the exocrine pancreas. Related to Fig.2.

Representative microscopical pictures from immunostainings of pancreatic sections from controls (n=5), AAb$^+$ (n=5) and T1D donors (n=5) triple-stained for viral RNA, amylase and DAPI or quadruple-stained for viral RNA, amylase, CD45 and DAPI. Magnification of viral RNA$^+$/amylase$^+$ cells as well as an RNA$^+$/amylase$^+$ cell next to a CD45$^+$ cell (lower right panel), which shows a typical CD45$^+$ close to a viral RNA$^+$ cell. Stainings were performed in two technical replica. Scale bar depicts 10µm.

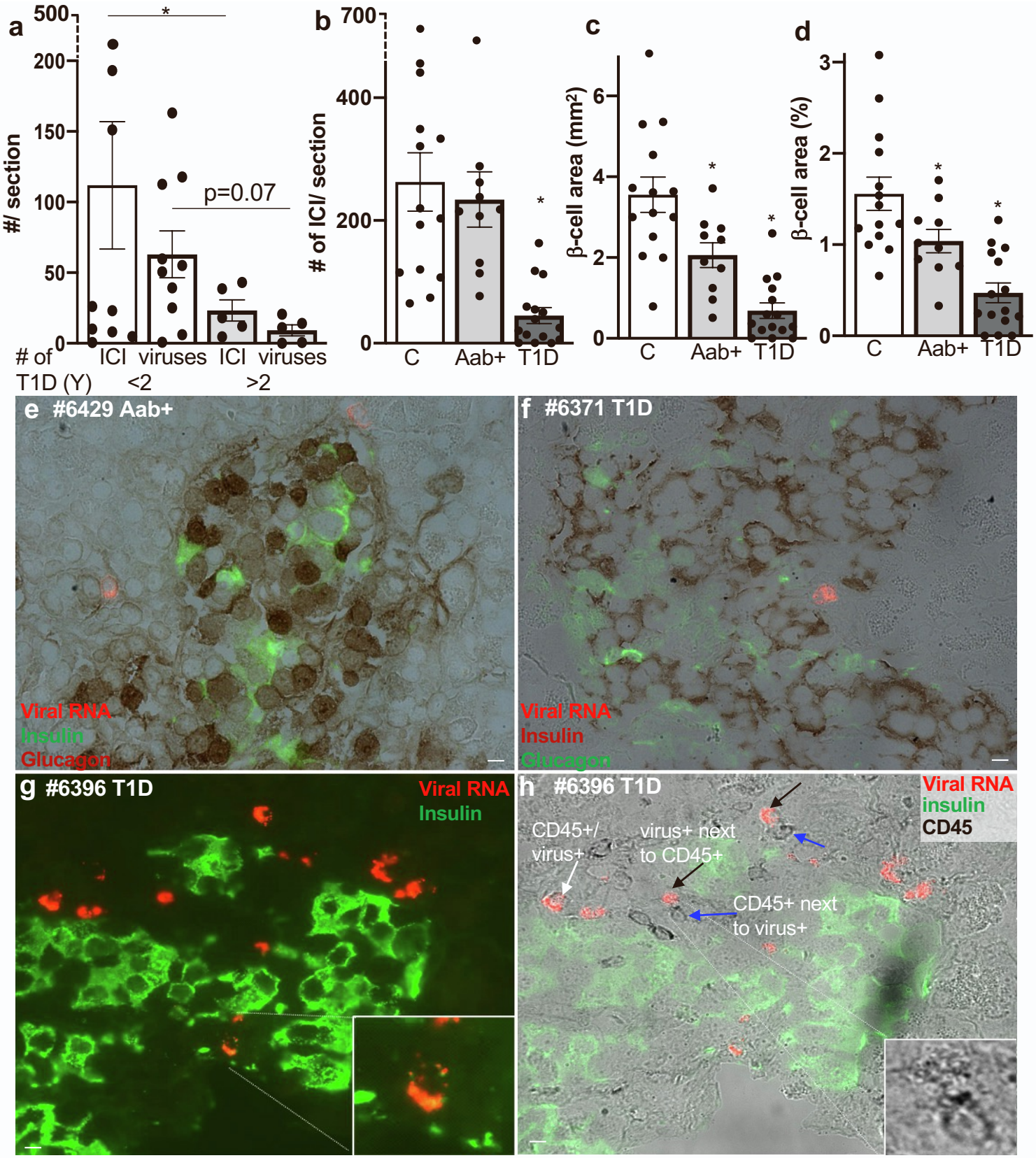

Supplemental Figure 3. Enteroviral RNA within islets. Related to Fig.2.

(A) The mean number of remaining insulin containing islets (ICIs) as well as virus-infected cells (as presented in Figure 1a) were counted manually throughout the whole pancreas sections and donors were grouped in short (<2 years) and long (>2 years) T1D disease duration (n=15). **(B)** The mean number of remaining insulin containing islets (ICIs) throughout the whole pancreas sections from all donors and **(C)** the area of all insulin containing islets expressed in mm^2. **(D)** The mean percentage of the β-cell area per pancreas was calculated from the ratio of insulin-positive to whole pancreatic tissue area. **(E-H)** Representative microscopical pictures from immunostainings of AAb^+ **(E)** and T1D **(F-H)** pancreatic sections of insulin containing islets triple-stained for viral **(E,F)** RNA, insulin and glucagon or **(G,H)** for viral RNA, CD45 and insulin. Magnification of viral RNA^+ cells with their typical disrupted morphology is shown **(H).** White arrow shows a viral $RNA^+/CD45^+$ co-positive cell, black arrow viral $RNA^+/CD45^-$ cell and blue arrow viral $RNA^-/CD45^+$ cells. Stainings were performed in two technical replica from control (n=14), AAb^+ (n=10) and T1D (n=15) donors; scale bars depicts 10µm.

Suppl.Table 1. Number of viral mRNA positive cells in the pancreas. Related to Fig.1. Mean number of all viral mRNA positive cells/slide in each donor throughout the pancreas and separated in cells with the appearance of ≥10 (full grade infection) or 1-9 single puncta per cell (low grade infection)

	ID	type	Virus (n)	full grade(≥10)	low grade (<10)
1	6104-02	control	0	0	0
2	6375-01	control	0	0	0
3	6413-02	control	0	0	0
4	6278-04	control	0	0	0
5	6102	control	0	0	0
6	6384-02	control	1	1	0
7	6254-02	control	2	2	0
8	6406-02	control	4	4	0
9	6238-02	control	7	6	1
10	6401-02	control	10	7	3
11	6339	control	4	3	1
12	6182	control	7	3	4
13	6030	control	7	3	4
14	6103	control	11	6	5
MEAN			**3.7**	**2.5**	**1.3**
1	6421-02	Aab+	1	1	0
2	6400-02	Aab+	3	3	0
3	6429-02	Aab++	61	54	7
4	6424-0	Aab++	249	223	26
5	6301	Aab+	0	0	0
6	6397	Aab+	1	1	0
7	6303	Aab+	4	4	0
8	6388	Aab++	5	5	0
9	6310	Aab+	27	24	3
10	6347	Aab+	360	329	31
MEAN			**71**	**64**	**7**
1	6299-04	T1D	18	16	2
2	6367-0	T1D	23	21	2
3	6396-02	T1D	193	146	47
4	6380-0	T1D	365	324	41
5	E560	T1D	151	133	18
6	6371-0	T1D	337	302	35
7	6211	T1D	43	42	1
8	6399	T1D	8	6	2
9	6414	T1D	5	2	3
10	6405	T1D	1	0	1
11	6070	T1D	5	4	1
12	6026	T1D	12	4	8
13	6209	T1D	10	8	2
14	6046	T1D	39	36	3
15	6362	T1D	26	23	3
MEAN			**82**	**71**	**11**

Suppl.Table 2. nPOD inventory donor case IDs and demographics. Related to Fig.1-3.

#	ID	type	Aab	Diab. Durat	age	gender	Ethnicity	C-pep (ng/ml)	HbA 1c	BMI	diabetes family history	Diagnosis
1	6104-02	control	neg.		41	male	Caucasian	20.6	n.a.	21	NO	anoxia
2	6375-01	control	neg.		29	male	Caucasian	17.3	5.7	32	YES	head trauma
3	6413-02	control	neg.		10	female	Caucasian	5.3	5.6	19	NO	head trauma
4	6278-04	control	neg.		12	female	afr.-am.	4.5	6.3	21	NO	anoxia
5	6102	control	neg.		45	female	Caucasian	0.6	6.1	35	YES	cerebrovascular
6	6384-02	control	neg.		17	male	Caucasian	0.7	4.8	18	NO	head trauma
7	6254-02	control	neg.		38	male	Caucasian	6.4	5.3	31	NO	anoxia
8	6406-02	control	neg.		7	male	Caucasian	4.1	5.1	17	NO	head trauma
9	6238-02	control	neg.		20	male	afr.-am.	1.2	n.a.	22	NO	head trauma
10	6401-02	control	neg.		25	female	hispanic	12.8	5.8	31	YES	head trauma
11	6339	control	neg.		23	male	Caucasian	10.6	5.3	25	YES	head trauma
12	6182	control	neg.		3	male	Caucasian	2.3	n.a.	26	NO	anoxia
13	6030	control	neg.		30	male	Caucasian	2.5	n.a.	27	n.a.	head trauma
14	6103	control	neg.		2	male	Caucasian	1.0	6.1	17	NO	anoxia
MEAN					**22**			**6.4**	**5.6**	**24**		
1	6421-02	Aab+	GADA		7	male	Hispanic	1.8	5.6	18	NO	head trauma
2	6400-02	Aab+	GADA		25	male	Hispanic	4.2	5.5	22	YES	head trauma
3	6429-02	Aab++	GADA mIAA		22	male	afr.-am.	2.3	5.5	20	NO	head trauma
4	6424-0	Aab++	GADA mIAA		18	male	Caucasian	7.0	5.8	51	YES	head trauma
5	6301	Aab+	GADA		26	male	afr.-am.	3.9	5.5	32	NO	head trauma
6	6397	Aab+	GADA		21	female	Caucasian	12.8	6.0	30	NO	head trauma
7	6303	Aab+	GADA		22	male	Caucasian	3.0	5.4	32	YES	head trauma
8	6388	Aab++	GADA mIAA		25	female	Hispanic	1.4	5.7	26	YES	anoxia
9	6310	Aab+	GADA		28	female	Hispanic	10.5	n.a.	22	YES	anoxia
10	6347	Aab+	mIAA		9	male	Caucasian	3.3	n.a.	20	YES	head trauma
MEAN					**20**			**5.0**	**5.6**	**27**		
1	6299-04	T1D	mIAA	23	32	male	Caucasian	<0.05	n.a.	32	NO	anoxia
2	6367-0	T1D	neg.	2	24	male	Caucasian	0.4	8.8	26	YES	anoxia
3	6396-02	T1D	neg.	2	17	female	Caucasian	0.1	13.4	23	YES	DKA, cerebral edema
4	6380-0	T1D	neg.	0	12	female	afr.-am.	0.2	13.5	15	YES	DKA, cerebral edema
5	E560	T1D	n.d.	1.5	42	female						UK cohort panc.
6	6371-0	T1D	GADA, IA-2A mIAA, ZnT8A	2	13	female	Caucasian	0.1	9.5	17	YES	cerebral edema
7	6211	T1D	GADA, IA-2A mIAA, ZnT8A	4	24	female	afr.-am.	<0.05	10.5	24	NO	anoxia
8	6399	T1D	GADA, IA-2A ZnT8A	0	17	male	Caucasian	1.4	10.4	32	NO	anoxia
9	6414	T1D	GADA, mIAA ZnT8A	0.4	23	male	afr.-am.	0.2	14.0	28	YES	anoxia
10	6405	T1D	GADA, IA-2A ZnT8A	0.6	29	female	Hispanic	1.8	7.0	43	NO	cerebrovascular
11	6070	T1D	IA-2A mIAA	7	23	female	Caucasian	<0.05	n.a.	22	NO	anoxia
12	6026	T1D	mIAA	9	22	male	Caucasian	<0.05	n.a.	24	YES	head trauma
13	6209	T1D	IA-2A mIAA, ZnT8A	0.25	5	female	Caucasian	0.1	n.a.	16	NO	DKA, cerebral edema
14	6046	T1D	IA-2A ZnT8A	8	19	female	Caucasian	<0.05	n.a.	25	NO	anoxia
15	6362	T1D	GADA	0	25	male	Caucasian	0.4	10.0	29	YES	head trauma
MEAN				**4**	**22**			**0.4**	**10.8**	**25**		

Suppl.Table 3. HLA A, B, DRB1 and DQB1 alleles of the nPOD donors studied and mean number of viral mRNA positive cells/pancreas slide from each donor. Related to Fig.1-3.

#	ID	type	HLA-A (1st allele)	HLA-A (2nd allele)	HLA-B (1st allele)	HLA-B (2nd allele)	HLA-DRB1 (1st allele)	HLA-DRB1 (2nd allele)	HLA-DQA1 (1st allele)	HLA-DQA1 (2nd allele)	HLA-DQB1 (1st allele)	HLA-DQB1 (2nd allele)	#virus$^+$ cells/ panc. slide
1	6104-02	control	29:02	68:01	39:06	44:03	07:01	13:01	02:01	01:01	02:01	05:01	0
2	6375-01	control	02:01	29:02			04:01	14:01	03:01	01:01	03:02	05:03	0
3	6413-02	control	01:01	02:01	08:01	51:01	01:01	03:01	01:01	05:01	05:01	02:01	0
4	6278-04	control	23:01	68:02			11:04	12:01	05:01	03:01	05:02	03:01	0
5	6102	control	03:01	31:01	08:01	44:02	03:01	04:01	05:01	03:01	02:01	03:01	0
6	6384-02	control	24:02	69:01			11:01	15:01	05:03	01:02	06:02	03:01	1
7	6254-02	control	02:01	29:02			03:01	07:01	05:01	02:01	02:02	02:01	2
8	6406-02	control	02:01	11:01	44:03	51:08	03:01	07:01	05:01	02:01	02:01	02:02	4
9	6238-02	control	02:05	32:01			03:02	11:01	04:01	05:01	04:02	03:01	7
10	6401-02	control	31:01	33:03	14:02	51:01	07:01	13:01	01:03	01:02	06:03	02:02	10
11	6339	control	01:01	02:01			03:01	10:01	01:01	05:01	02:01	05:01	4
12	6182	control	02:01	03:01			04:01	16:02	03:01	01:02	03:01	05:02	7
13	6030	control	02:01	31:01	07:02	44:03	07:01	15:01	02:01	01:02	02:01	06:02	7
14	6103	control	02:01	80:01	40:02	44:02	11:01	13:01	05:01	01:03	03:01	06:03	11
1	6421-02	Aab+	02:01	03:01	15:01	27:05	01:01	01:01	01:01	01:01	05:01	05:01	1
2	6400-02	Aab+	26:01	31:01			04:07	13:04	03:01	05:05	03:02	03:19	3
3	6429-02	Aab+	01:01	02:01	44:02	81:01	01:03	03:01	01:01	05:01	05:01	02:01	61
4	6424-0	Aab+	30:01	68:01	08:01	35:03	03:01	04:01	05:01	03:01	02:01	03:02	249
5	6301	Aab+	23:01	23:01			11:01	13:04	05:01	01:02	03:19	06:02	0
6	6397	Aab+	02:01	02:01			13:01	15:01	01:03	01:02	06:03	06:02	1
7	6303	Aab+	01:01	11:01			03:01	07:01	05:01	02:01	02:01	02:02	4
8	6388	Aab+	02:01	02:01			01:02	04:07	01:01	03:01	05:01	03:01	5
9	6310	Aab+	03:01	30:01			07:01	11:02	02:01	05:01	02:02	03:19	27
10	6347	Aab+	02:01	32:01			01:01	15:01	01:01	01:02	05:01	06:02	360
1	6299-04	T1D	01:01	11:01			03:01	04:01	05:01	03:01	02:01	03:02	18
2	6367-0	T1D	02:01	29:02			04:01	07:01	02:01	03:01	02:01	11:01	23
3	6396-02	T1D	23:01	24:02			03:01	07:01	05:01	02:01	02:01	02:02	193
4	6380-0	T1D	33:02	68:02			03:01	13:02	05:01	01:02	02:01	06:04	365
5	E560												151
6	6371-0	T1D	01:01	68;02			03:01	13:02	05:01	01:02	02:01	06:04	337
7	6211	T1D	02:01	03:01			04:05	12:01	03:01	05:01	03:02	03:01	43
8	6399	T1D	02:01	03:01			09:01	15:01	03:02	01:02	03:03	06:02	8
9	6414	T1D	01:01	23:01	07:02	08:01	03:01	09:01	05:01	03:03	02:01	02:02	5
10	6405	T1D	30:02	31:01	18:01	40:02	03:01	04:07	05:01	03:01	02:01	03:02	1
11	6070	T1D	02:01	02:05	38:01	58:01	10:01	16:01	01:01	01:02	05:01	05:02	5
12	6026	T1D	01:01	24:02	08:01	18:01	03:01	13:02	01:02	05:01	06:04	02:01	12
13	6209	T1D	01:01	02:01			03:01	04:01	03:01	05:01	03:02	02:01	10
14	6046	T1D	02:01	03:01	15:01	39:01	01:01	04:01	01:01	03:01	05:01	03:02	39
15	6362	T1D	03:01	11:01			01:03	03:01	01:01	05:01	05:01	02:01	26